Probabilistic Treatment of Crack Nucleation and Growth for Gas Turbine Engine Materials

M. P. Enright

R. C. McClung

S. J. Hudak

W. L. Francis

Southwest Research Institute,
San Antonio, TX 78238

The empirical models commonly used for probabilistic life prediction do not provide adequate treatment of the physical parameters that characterize fatigue damage development. For these models, probabilistic treatment is limited to statistical analysis of strain-life regression fit parameters. In this paper, a model is proposed for life prediction that is based on separate nucleation and growth phases of total fatigue life. The model was calibrated using existing smooth specimen strain-life data, and it has been validated for other geometries. Crack nucleation scatter is estimated based on the variability associated with smooth specimen and fatigue crack growth data, including the influences of correlation among crack nucleation and growth phases. The influences of crack nucleation and growth variability on life and probability of fracture are illustrated for a representative gas turbine engine disk geometry. [DOI: 10.1115/1.4000289]

1 Introduction

Probabilistic damage tolerance (PDT) is becoming an established practice for risk assessment of high-energy rotating components in commercial aircraft gas turbine engines. Although the existing safe-life approach is an accepted practice for nominal conditions [1], it does not address out-of-condition inherent and induced anomalies such as the ones that led to the incidents in Sioux City, IA [2] and Pensacola, FL [3], respectively. A PDT is summarized in a recent Federal Aviation Administration (FAA) Advisory Circular [1] that provides guidance on the assessment of the risk of fracture associated with inherent anomalies in titanium rotors. Further details regarding PDT methodologies for gas turbine engines are provided in Refs. [4–10].

Some of the existing PDT methodologies predict the probability of fracture associated with populations of anomalies that form growing cracks during the first cycle of applied load (e.g., Refs. [6–10]). However, the crack nucleation life associated with some materials may be non-negligible [11,12] and must be considered in the risk computation. Furthermore, gas turbine engine materials are also vulnerable to cracks that can form due to fatigue crack nucleation in nominal material, in addition to those caused by anomalies.

Historically, an empirical approach has been used to predict fatigue crack initiation life with an emphasis on regression analysis of strain-life data associated with standard smooth specimens [13]. The crack size associated with the end of the "initiation" event and with the beginning of the "crack growth" event is often chosen as a standard value such as 0.030 in. (0.76 mm) [14]. However, the crack growth process certainly begins at much smaller crack sizes. Furthermore, conventional crack initiation models are sometimes not accurate when a significant stress gradient occurs over the length scale of this standard initiation crack size.

The empirical smooth-specimen-based crack initiation model also has a number of shortcomings when applied to probabilistic life prediction. Since no information is provided regarding the fundamental random variables, probabilistic treatment is limited to statistical analysis of the parameters associated with a regression fit of strain-life (failure) data. Although the combined contributions of the nucleation and growth scatter are reflected in the failure data, it is not possible to predict the relative magnitudes of the individual contributions solely based on strain-life results. The interaction among the nucleation and growth phases is not well understood, and the empirical model provides no guidance regarding this relationship.

In this paper, a fatigue nucleation and growth (FaNG) model is proposed for life prediction that is based on separate nucleation and growth phases of fatigue life. The relative contributions of these phases are quantified for a specified set of conditions (e.g., anomaly size, crack geometry, and stress range). The model was calibrated using existing smooth specimen strain-life data, and it has been validated for a notched geometry. Crack nucleation scatter is estimated based on the variability associated with experimental smooth specimen and fatigue crack growth data, including the influences of correlation among the crack nucleation and growth phases. The influences of crack nucleation and growth variability on life and probability of fracture are illustrated for a gas turbine engine disk.

2 Continuum Crack Nucleation Life Modeling

2.1 Deterministic Crack Nucleation Life. A new paradigm has been proposed for the development of fatigue life models, based on the summation of crack nucleation and crack growth life phases, with the transition occurring at a physically meaningful crack nucleation size [15]. This paradigm, illustrated in Fig. 1, can be applied to empirical models, micromechanical models, or physically informed engineering models. The paradigm employs the usual history information such as stress, strain, and temperature, but material information may include both traditional empirical properties as well as microstructure data. The three crack growth regimes shown may reduce to two regimes or even one regime for certain problems. The initial crack size for the growth analysis may be random (e.g., defined in terms of a random microstructure), fixed, or dependent on the nucleation and/or growth models. Typically, the initial crack size will be much smaller than the traditional 0.030 in. flaw often used at the start of a conventional damage tolerance analysis.

The application of the paradigm to conventional empirical life models is illustrated in Fig. 2. Traditional "crack initiation" models (strain-life or stress-life) commonly characterize the number of cycles required to fracture a smooth cylindrical specimen, and some portion of this life is obviously crack growth. It is conceptually straightforward to back-calculate the crack growth fraction

Contributed by the Manufacturing Materials and Metallurgy Committee of ASME for publication in the JOURNAL OF ENGINEERING FOR GAS TURBINES AND POWER. Manuscript received May 14, 2009; final manuscript received June 5, 2009; published online May 26, 2010. Editor: Dilip R. Ballal.

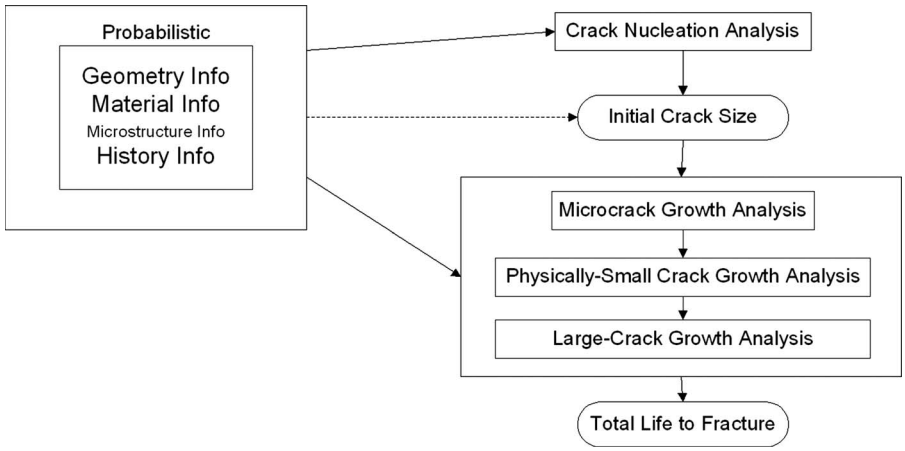

Fig. 1 A proposed FaNG model addresses the different phases of fatigue damage development

of the total smooth specimen life for some specified "little" crack size using fracture mechanics models, thereby deriving a true nucleation life curve for that crack size. This nucleation curve can then be applied to determine the crack nucleation life for other configurations based on the equivalence of the local stresses at the crack nucleation site. The total life to failure for the new configuration can be calculated by summing this nucleation life with the crack propagation life calculated from the nucleation crack size. This construction permits a direct treatment of the damage growth mechanisms at various crack sizes, which may be especially important for significant stress gradients. The construction also permits a realistic assessment of crack nucleation versus crack growth contributions to total life.

2.2 Smooth Specimen Life Variability. Smooth specimen fatigue life is often presented in a strain-life format that is based on a regression analysis of experimental test data. For example, the Smith–Watson–Topper (SWT) model [16] is expressed as

$$f(2N_f) = \sigma_{\max}\frac{\Delta\varepsilon}{2} = \frac{\sigma_f'^2}{E}(2N_f)^{2b} + \sigma_f'\varepsilon_f(2N_f)^{b+c} \tag{1}$$

where

$$\sigma_{\max} = \frac{\Delta\sigma}{2} + \sigma_{\text{mean}} \tag{2}$$

The SWT model includes terms associated with elastic strain ε_e and plastic strain ε_p values, Eqs. (3) and (4), respectively. The coefficients and exponents for the terms in Eqs. (3) and (4) are obtained from the linear regression of strain-life data in the log-log space

$$\frac{\Delta\varepsilon_e}{2} = \frac{\sigma_f'}{\mathrm{E}}(2N_f)^b \tag{3}$$

$$\frac{\Delta\varepsilon_p}{2} = \varepsilon_f'(2N_f)^c \tag{4}$$

The standard error associated with linear regression is given by [17]

$$s_{X|y}^2 = \frac{1}{n-2}\sum_{i=1}^{n}(x_i - x_i')^2 \tag{5}$$

where n is the number of experimental data values, and x_i and x_i' are the horizontal coordinates of the experimental and regression data, respectively. However, since the regression is performed in the log-log space, Eq. (5) becomes

$$s^2_{\log(2N_e)} = \frac{1}{n_e-2}\sum_{i=1}^{n_e}[\log(2N_e) - \log(2N_e')]^2 \tag{6}$$

for the life N_e associated with elastic strain, and

$$s^2_{\log(2N_p)} = \frac{1}{n_p-2}\sum_{i=1}^{n_p}[\log(2N_p) - \log(2N_p')]^2 \tag{7}$$

for the life N_p associated with plastic strain. Noting that Eq. (1) is a linear combination of Eqs. (3) and (4), if it is assumed that the logarithm of the lives associated with elastic and plastic strains are perfectly correlated, then the variance associated with Eq. (1) can be expressed as [18]

$$s^2_{\log(2N_f)} = s^2_{\log(2N_e)} + s^2_{\log(2N_p)} + 2s_{\log(2N_e)}s_{\log(2N_p)} \tag{8}$$

The confidence interval associated with the smooth specimen life N_f at a specified stress range value is obtained by applying k_α to the logarithm of N_f

$$\log(2N_{f,\text{c.i.}}) = \log(2N_f) \pm k_\alpha s_{\log(2N_f)} \tag{9}$$

where k_α is the standard normal variate associated with a $(1-\alpha)$ confidence interval.

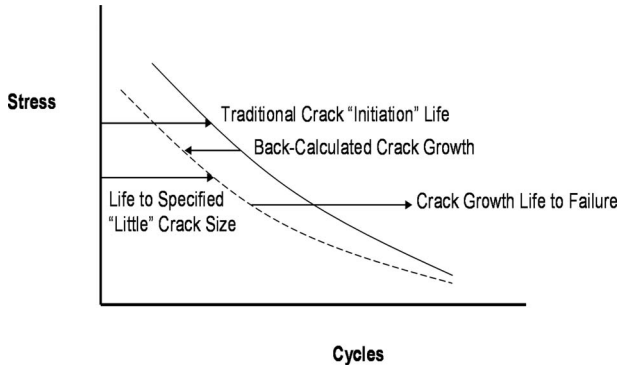

Fig. 2 The FaNG model predicts the nucleation life portion of smooth specimen life associated with a specific initial crack size

2.3 Crack Nucleation Life Variability. The FaNG model is defined as the linear combination of crack nucleation and growth terms:

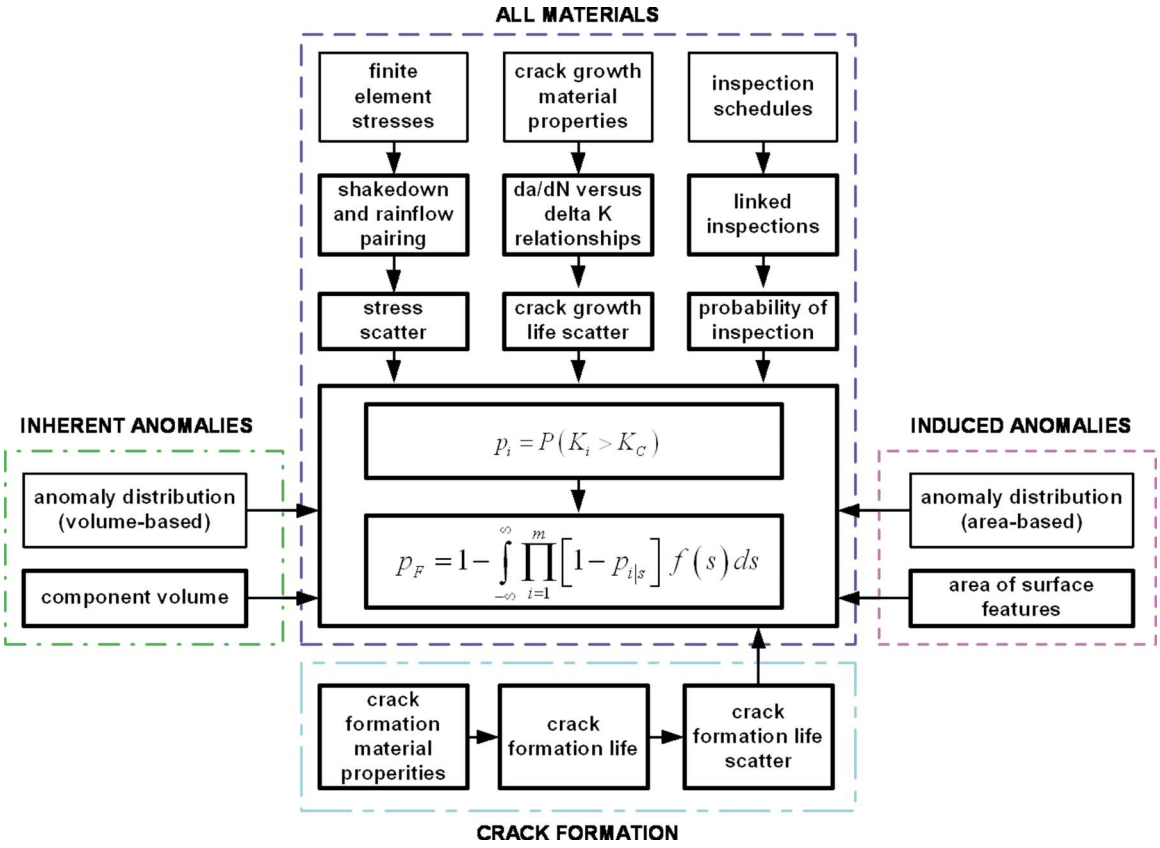

Fig. 3 A probabilistic framework has been developed to predict the fracture risk associated with crack nucleation and growth [19]

$$N_f = N_f^n + N_f^p \tag{10}$$

where N_f^n and N_f^p represent the nucleation and growth portions of total (smooth specimen or crack initiation) life, respectively. First order estimates of the mean μ_{N_f} and standard σ_{N_f} deviations of total life are given by [18]

$$\mu_{N_f} \cong E(N_f^n) + E(N_f^p) \tag{11}$$

$$\sigma_{N_f}^2 \cong \sigma_{N_f^n}^2 + \sigma_{N_f^p}^2 + 2\rho_{N_f^n N_f^p}\sigma_{N_f^n}\sigma_{N_f^p} \tag{12}$$

The variability associated with the nucleation portion of total life is obtained by solving Eq. (12) for $\sigma_{N_f^n}$

$$\sigma_{N_f^n} = \frac{1}{2}\left[\begin{array}{l} -2\rho_{N_f^n N_f^p}\sigma_{N_f^p} \pm \\ \sqrt{(2\rho_{N_f^n N_f^p}\sigma_{N_f^p})^2 - 4(\sigma_{N_f^p}^2 - \sigma_{N_f}^2)} \end{array}\right] \tag{13}$$

The nucleation and growth models are typically linear when presented in the log-log or ln-ln space. The mean and variance of the total life in the ln-ln space are

$$\lambda_{N_f} = \ln[\mu_{N_f}] - \tfrac{1}{2}\zeta_{N_f}^2 \tag{14}$$

and

$$\zeta_{N_f}^2 = \ln\left[1 + \left(\frac{\sigma_{N_f}}{\mu_{N_f}}\right)^2\right] \tag{15}$$

The confidence interval associated with total life in the ln-ln space can be expressed as

$$\ln(N_{f,\text{c.i.}}) = \lambda_{N_f} \pm k_\alpha \zeta_{N_f} \tag{16}$$

or

$$N_{f,\text{c.i.}} = \exp\left[\ln(\mu_{N_f}) - \tfrac{1}{2}\zeta_{N_f}^2 \pm k_\alpha \zeta_{N_f}\right] \tag{17}$$

The probability of fracture associated with the combined nucleation and growth models can be expressed as

$$P(N \le N_s) = \Phi\left[\frac{\ln(N_s) - \lambda_{N_f}}{\zeta_{N_f}}\right] \tag{18}$$

where N_s is the service life and Φ is the cumulative distribution function (CDF) associated with the standard normal probability density function.

3 Probabilistic Framework for Crack Nucleation and Growth

A general probabilistic framework has been developed for risk assessment of gas turbine engine components [19]. It includes random variables associated with applied loads, crack growth life, inherent and induced material anomalies, and inspection-related variables. Additional random variables are included to address crack nucleation. As shown in Fig. 3, the framework provides probabilistic treatment of both inherent and induced anomalies using a general equation that is common to several material types.

The crack growth life is highly dependent on the size of the initial crack, which is treated as a random variable. The probability of fracture at a specified crack location is modeled as the likelihood that a random anomaly is larger than a critical size d^*, where d^* is the size of an anomaly that leads to failure within the specified service life [20,21]

$$p_{i|L_G,s} f(l_G) = P(d < d^* | l_G, s) \tag{19}$$

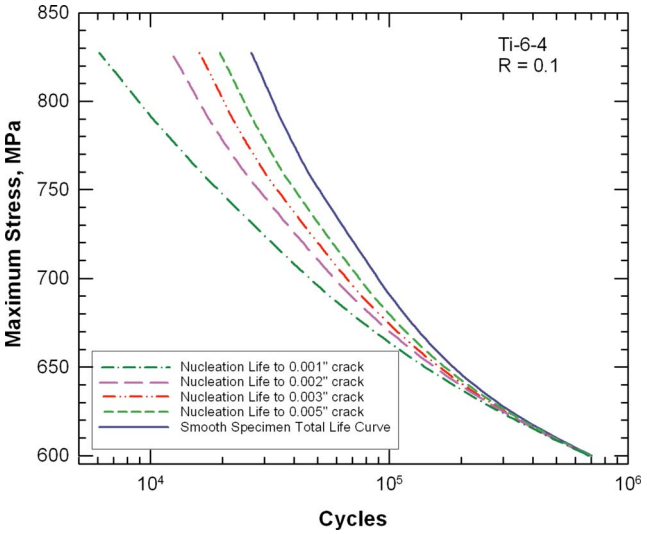

Fig. 4 Predicted nucleation life for a smooth specimen at various definitions of the crack nucleation size

The crack growth life is also influenced by the anomaly occurrence rate λ and the variability associated with the crack growth life L_G. When these influences are included, Eq. (19) becomes

$$p_{i|s}(s) = 1 - \exp\left\{-\lambda\left[1 - \int_{-\infty}^{\infty} p_{i|L_G,s} f_{L_G}(l_G) dl_G\right]\right\} \quad (20)$$

Anomalies may be located anywhere within a component. For risk predictions, the component is subdivided into a number of subregions or zones each containing one or more anomalies. Component risk is modeled as a series system of m zones. In addition, variability associated with applied stress values is addressed by introducing a stress scatter random variable S

$$p_F = 1 - \int_{-\infty}^{\infty} \prod_{i=1}^{m} [1 - p_{i|s}] f(s) ds \quad (21)$$

4 Application of Crack Nucleation Models to Titanium Alloys

4.1 Deterministic Crack Nucleation Life (Smooth Specimens). A fatigue crack nucleation and growth model [15] was constructed for Ti–6Al–4V smooth specimens and implemented in DARWIN® [6–10]. The model estimates the number of fatigue cycles required to form a crack of some small, user-defined size by calculating the number of cycles required to grow a crack of this initial size to failure in a smooth specimen geometry, and then subtracting this total from the observed total smooth specimen fatigue life. The model includes small-crack effects and stress-level effects.

The estimated crack nucleation lives to various crack sizes for a smooth specimen are shown in Fig. 4 for $R=0.1$, along with the smooth specimen total life. The nucleation lives were determined by calculating the crack growth life to failure from the specified initial crack size in a smooth specimen, based on a modified Smith–Watson–Topper representation of the smooth specimen data, a tabular representation of the large-crack growth rate data, and a simple small-crack model [22]. Similar calculations can be performed at other stress ratios.

The predicted fraction of the total smooth specimen life consumed by crack nucleation is shown in Fig. 5 for different definitions of the crack nucleation size and different cycles to failure (stress amplitudes) at a fixed stress ratio ($R=0.1$). The nucleation life fraction is a function of both nucleation crack size and total life, increasing to nearly 100% at long lifetimes (low applied stresses) for all nucleation sizes.

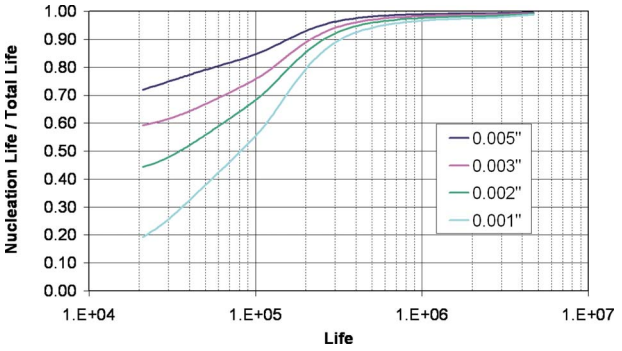

Fig. 5 Predicted nucleation life fraction for a smooth specimen at various definitions of the crack nucleation size

4.2 Deterministic Crack Nucleation Life (Notched Specimens). The FaNG model was then adapted for application to notched geometries. The model calculates the total fatigue life in two steps. In the first step, a crack nucleation life corresponding to a specified nucleation length is calculated. This step employs the same crack nucleation model used previously for smooth specimens. However, the characteristic formation stress in the model is no longer the uniform stress applied to the smooth specimen. Instead, the characteristic nucleation stress is selected to be equal to the local stress in the stress concentration field at the nucleation length. If the nucleation length is 0.002 in. (0.005 cm), for example, the characteristic nucleation stress is taken to be the stress 0.002 in. (0.005 cm) inside the surface of the stress concentration. This characteristic nucleation stress is applied to the "smooth specimen" model as if the entire smooth specimen was subjected to a uniform stress of this magnitude.

The second step in the total life calculation is to perform a fatigue crack growth life calculation for a surface crack at a stress concentration, starting with the specified crack nucleation size and terminating at fracture. This second step is completely independent of the smooth specimen calculations in the first step, except that the crack nucleation size employed in the first step is the starting crack length for the second step.

The model was applied to a series of double-edge notch fatigue tests that had been performed with the same Ti–6Al–4V material for two notch geometries and four nominal stress ratios [23]. One specimen (the so-called "V-notch" or "small volume" configuration) had a notch depth of 0.047 in. (0.119 cm), a notch root radius of 0.021 in. (0.053 cm), and a thickness of 0.142 in. (0.361 cm), while the other specimen ("U-notch" or "large volume") had a notch depth of 0.032 in. (0.081 cm), a notch root radius of 0.032 in. (0.081 cm), and a thickness of 0.250 in (0.635 cm). The nominal (net-section) stress concentration factor was approximately 2.5 for both geometries. The test reports indicated that most of the observed failures could be attributed to a single dominant semi-elliptical surface crack initiated near the center of the notch root.

If the elastic maximum stress in the notched specimen was calculated to be greater than the yield, then the DARWIN shakedown algorithm was invoked to calculate the elastic-plastic stress relaxation and redistribution at (and near) the notch root. When shakedown occurred, the local stress ratio was (in general) different from the nominal (applied) stress ratio, and the actual local stress ratio was considered in both the crack formation and growth life calculations. The cyclic stress-strain properties of Ti–6Al–4V were employed in the shakedown calculations.

Results for the total fatigue life calculations at $R=0.1$ are shown for the V-notch specimen in Fig. 6. The FaNG model predictions are compared with the actual test results and with predictions based on the SWT model normalized by the nominal stress concentration factor. A nucleation depth of 0.003 in. (0.008 cm)

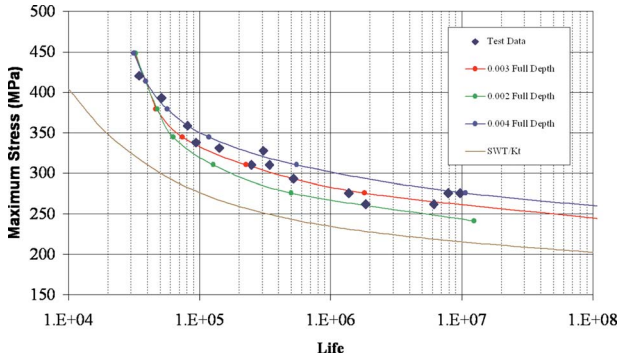

Fig. 6 Comparison of FaNG model (for different crack nucleation sizes) and normalized SWT predictions with R=0.1 notch fatigue test data

generally gave the best predictions in comparison to the other two values considered (0.002 in. (0.005 cm) and 0.004 in. (0.010 cm)). The normalized SWT predictions were very conservative.

Predictions for three different stress ratios are summarized in Fig. 7, considering only the 0.003 in. (0.008 cm) definition of nucleation stress. The agreement between test and model is generally strong under all conditions. It should be emphasized that the predictions shown here are not a fit to the notch test data (other than the selection of a common nucleation depth) because the material constants were derived only from smooth specimen and fracture mechanics tests. The predicted nucleation life fractions (predicted nucleation life to the specified nucleation crack size as a fraction of predicted total life) for the three stress ratios are summarized graphically in Fig. 8. As for the smooth specimens (Fig. 5), nucleation life fractions are smaller at shorter lives. The average nucleation life fraction is around 70% at a total life of 10^5 cycles, and the values do not change substantially with stress ratio.

4.3 Crack Nucleation Life Variability. The crack nucleation variability model was applied to the smooth specimen total life data [23] shown in Fig. 9. The mean smooth specimen life was identified from a nonlinear regression fit of the data [23]. The variance was computed directly using Eq. (6) and the nonlinear regression fit equation, with a resulting coefficient of variation (i.e., standard deviation/mean) value of 0.46 (for these computations, $2N_e$ was replaced with N_f). These results were applied to Eq. (9) to estimate the lower 95% confidence interval (also shown in Fig. 9).

Crack growth life scatter can be traced to variability in the crack growth rate values associated with a specific material, among other factors. For example, consider the variability in

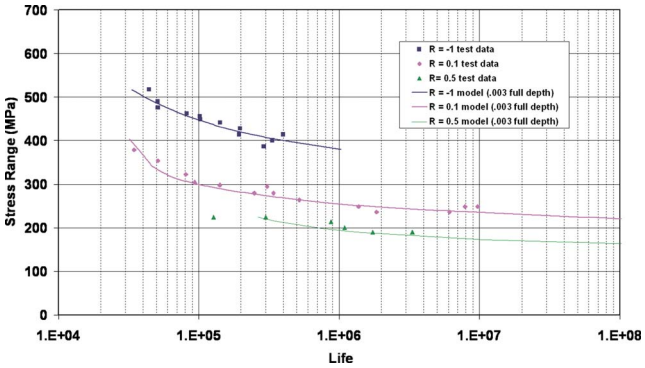

Fig. 7 Comparison of FaNG model predictions (crack nucleation size=0.003 in.) with notch fatigue test data for three different stress ratios

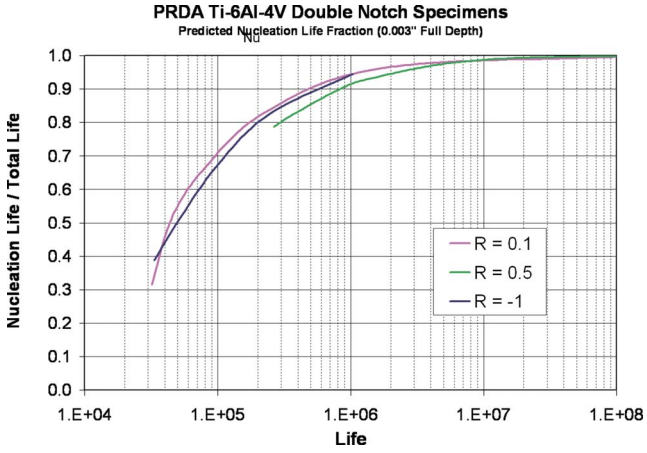

Fig. 8 Predicted crack nucleation life fractions based on the FaNG model for notch fatigue specimens at three different stress ratios

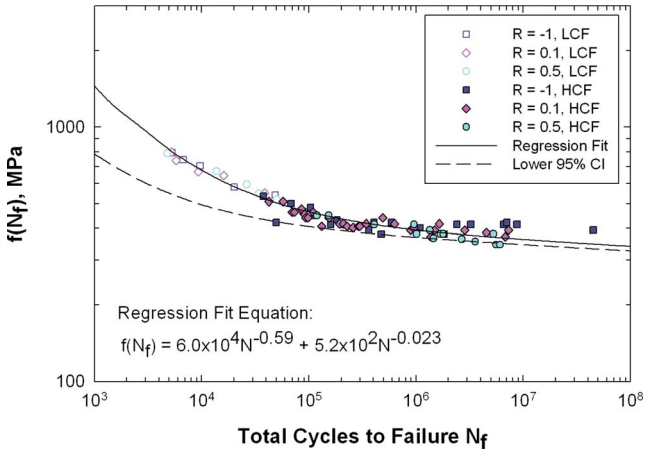

Fig. 9 Crack initiation lives and associated nonlinear regression equation for Ti–6Al–4V smooth specimen data [24]

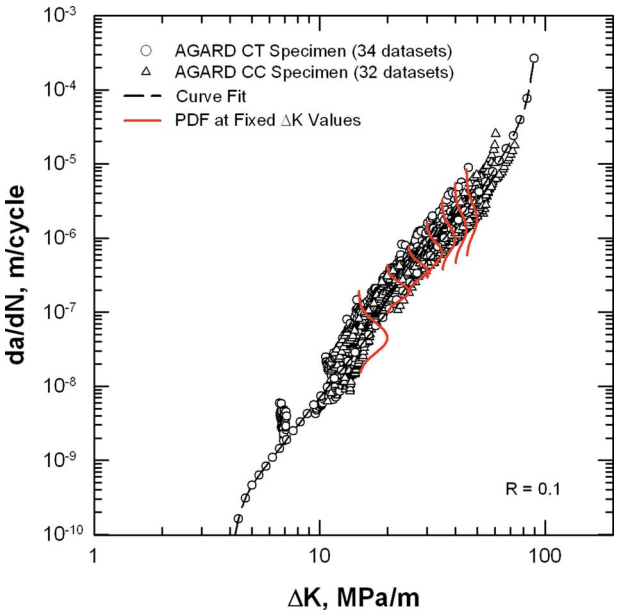

Fig. 10 Ti–6Al–4V crack growth rate data [24,25] and associated probability densities illustrate the dependence of da/dN variability on ΔK

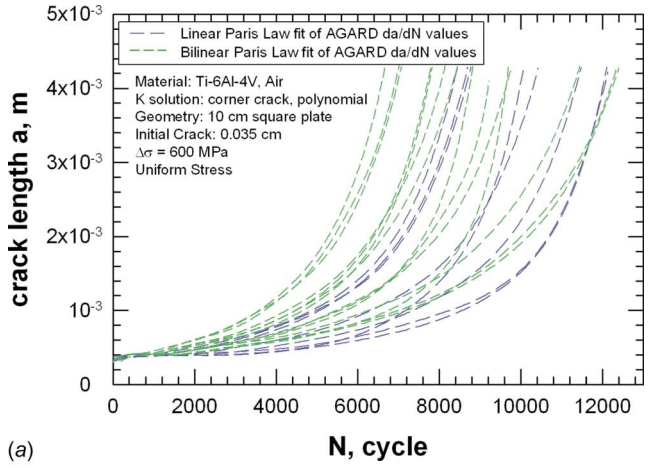

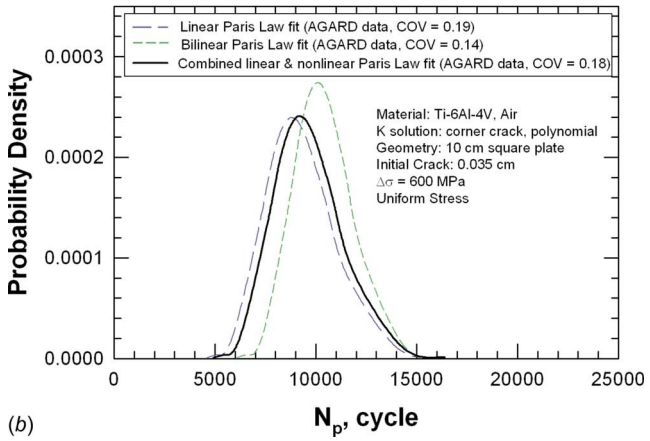

Fig. 11 Crack growth lives based on data from the AGARD study [24,25] were used to estimate Ti–6Al–4V crack growth life variability: (*a*) crack growth life results based on individual specimens and (*b*) crack growth life probability density

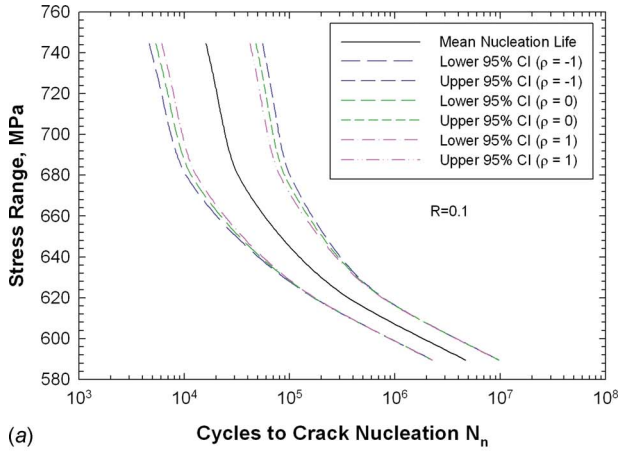

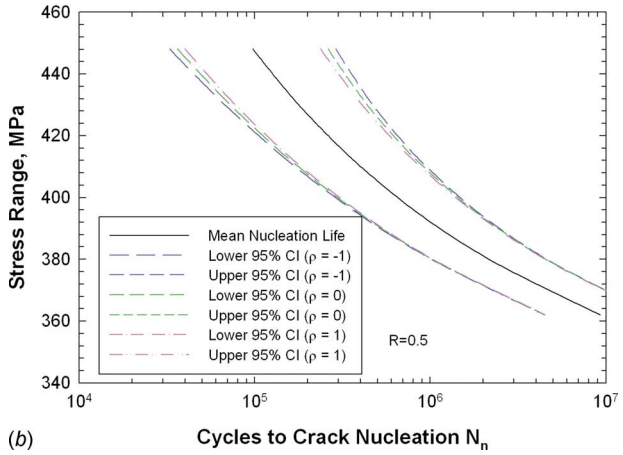

Fig. 12 Influence of correlation among crack nucleation and growth portions of crack initiation life on crack nucleation life confidence intervals: (*a*) *R*=0.1 and (*b*) *R*=0.5

da/dN values for titanium alloys associated with Advisory Group for Aerospace Research and Development (AGARD) experiments [24,25] shown in Fig. 10. It can be observed that the da/dN variability is dependent on ΔK. Crack growth life values (Fig. 11(*a*)) were estimated by numerically integrating crack growth rate curves based on linear and bilinear fits of individual specimens from this database, using an initial crack size of 0.035 cm and an applied stress range of 600 MPa. Probability densities associated with the crack growth life values are shown in Fig. 11(*b*). The resulting coefficient of variation (COV) value was 0.18 for crack growth life values associated with the combined linear and bilinear data sets.

The statistical relationship among crack nucleation and growth life is strongly influenced by material properties and applied loads. Material properties such as grain size introduce negative correlation among nucleation and growth lives, whereas applied loads introduce positive correlation. The confidence interval associated with smooth specimen nucleation life was computed using Eqs. (13) and (17) considering a range of values for the correlation among nucleation and propagation life values. The results are shown in Figs. 12(*a*) and 12(*b*) for $R=0.1$ and $R=0.5$, respectively. It can be observed that the confidence interval associated with $\rho_{N_f^n N_f^p}=-1$ is larger than those associated with the other correlation values. This represents the largest contribution of nucleation life variability to total life variability.

5 Application to Probabilistic Life Prediction of a Gas Turbine Engine Disk

The smooth specimen-based crack nucleation model was applied to life prediction of a gas turbine engine hub component

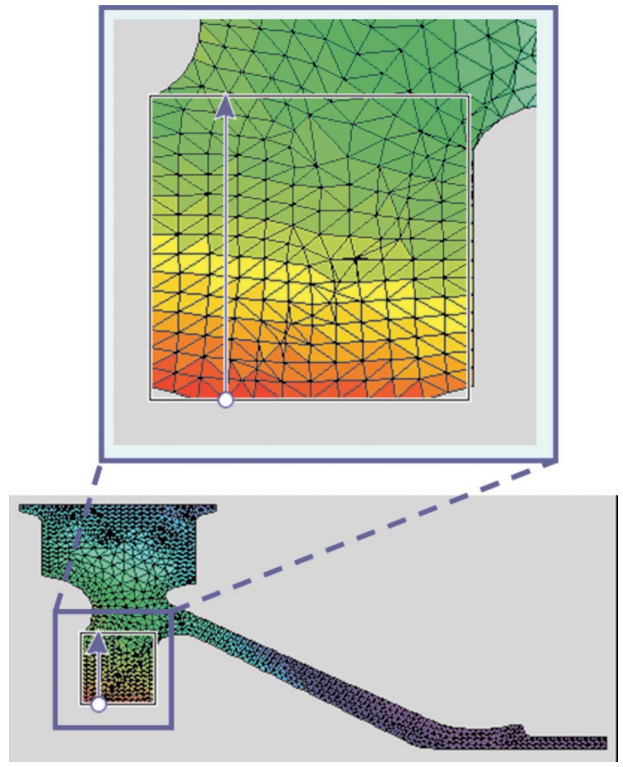

Fig. 13 The FaNG model was applied to risk assessment of an aircraft gas turbine engine disk

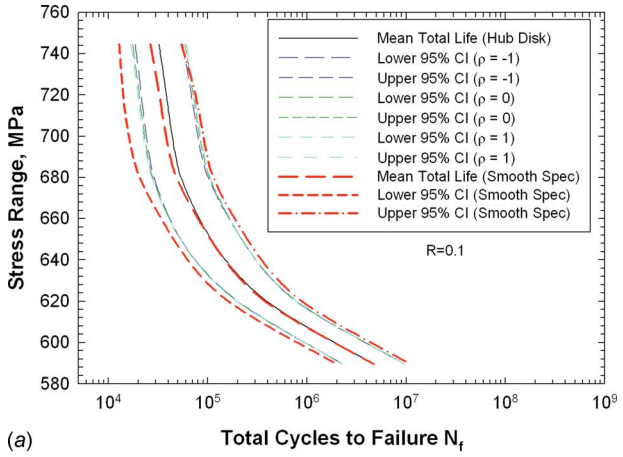

(*a*)

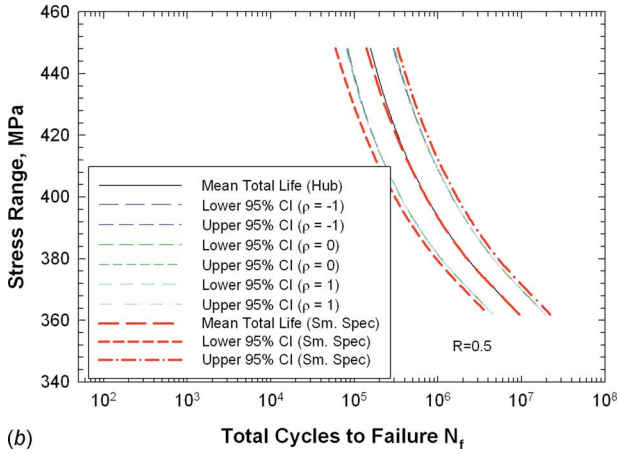

(*b*)

Fig. 14 For the gas turbine engine disk, predicted life values based on the FaNG model are generally higher than the smooth-specimen-based SWT model, particularly at relatively high stress range values: (*a*) *R*=0.1 and (*b*) *R*=0.5

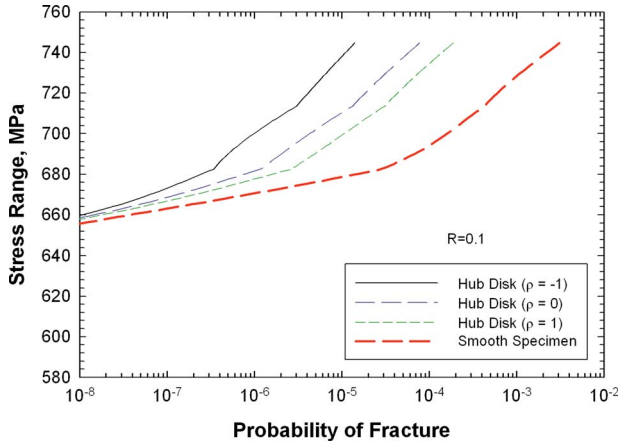

Fig. 15 A comparison of fracture probability values associated with FaNG and smooth-specimen-based SWT models indicates that FaNG predictions may be under- or overconservative depending on the stress range value and on the relationship among nucleation and growth lives

shown in Fig. 13. The crack growth life was estimated using a surface crack in plate stress intensity solution [26] and material parameters associated with the smooth specimen data. The mean total life was estimated using Eq. (11), and the total life variability was computed using Eq. (12) using the nucleation and growth COV values described in Sec. 4.3.

Total life results for stress range values applied at the surface of the hub disk are shown in Figs. 14(*a*) and 14(*b*) for $R=0.1$ and $R=0.5$, respectively. At low cycles, the predicted mean nucleation life is somewhat longer than the mean smooth specimen life, due to the less severe stress gradient of the hub compared with the uniform stress gradient associated with the smooth specimens. In general, the confidence intervals associated with the hub life predictions are narrower than those associated with the smooth specimen life, due to the increased ratio of propagation life and associated scatter. As this ratio increases, the total life scatter decreases, which also decreases the confidence interval. In contrast with Fig. 12, the confidence interval is larger for $\rho_{N_f^n N_f^p}=+1$ compared with other correlation values. Probability of fracture (P_f) values for the hub disk were identified using Eq. (18) with a service life of 8000 cycles, shown in Fig. 15. Predicted P_f values for the hub are one to two orders of magnitude smaller than the smooth specimen P_f values, and are strongly dependent on the correlation among nucleation and growth life values.

6 Conclusions

A probabilistic approach for fatigue life prediction was presented that addresses the variability associated with crack nucleation and growth phases of fatigue life. It is based on a new deterministic model that was developed to provide treatment of the significant stress gradients associated with these separate phases. The underlying deterministic model predicts the nucleation portion of life by subtracting calculated crack growth life (including small-crack corrections) in the smooth specimen from the total smooth specimen life. The resulting nucleation curves can be used to predict nucleation life to the same initial crack size in a feature of interest. Crack nucleation life variability is estimated based on smooth specimen and fatigue crack growth data, including the influences of correlation among the crack nucleation and growth phases. The model was applied to risk prediction of a representative gas turbine engine disk geometry. For the example disk considered, the predicted probability of fracture values were significantly lower compared with those based on the traditional strain-life approach.

Acknowledgment

This work was performed with funding from the U.S. Air Force Research Laboratory and the Southwest Research Institute under AFRL Dual Use Agreement No. F33615-03-2-5203. The support and encouragement of Jim Larsen, Jay Jira, and Patrick Golden (technical monitor) of AFRL are gratefully acknowledged.

References

[1] Federal Aviation Administration, 2001, "Advisory Circular—Damage Tolerance for High Energy Turbine Engine Rotors," U.S. Department of Transportation Paper No. AC33.14-1.
[2] National Transportation Safety Board, 1990, "Aircraft Accident Report—United Airlines Flight 232 McDonnell Douglas DC-10-10 Sioux Gateway Airport, Sioux City, Iowa, July 19, 1989," National Transportation Safety Board Report No. NTSB/AAR-90/06.
[3] National Transportation Safety Board, 1996, "Aircraft Accident Report—Uncontained Engine Failure, Delta Air Lines Flight 1288, McDonnell Douglas MD-88, N927DA," National Transportation Safety Board Report No. NTSB/AAR-98/01.
[4] Roth, P. G., 1992, "Probabilistic Rotor Design System (PRDS) Phase I," GE Aircraft Engines Paper No. WL-TR-92-2011.
[5] Adamson, J. D., Fox, E. P., and Malone, J. E., 1995, "Probabilistic Design System—Phase I and II Interim Report," Pratt and Whitney Report No. FR-24004-1.
[6] Leverant, G. R., 2000, "Turbine Rotor Material Design—Final Report," Federal Aviation Administration Report No. DOT/FAA/AR-00/64.
[7] Leverant, G. R., McClung, R. C., Millwater, H. R., and Enright, M. P., 2004, "A New Tool for Design and Certification of Aircraft Turbine Rotors," ASME J. Eng. Gas Turbines Power, **126**(1), pp. 155–159.
[8] McClung, R. C., Enright, M. P., Millwater, H. R., Leverant, G. R., and Hudak, S. J., 2004, "A Software Framework for Probabilistic Fatigue Life Assessment," J. ASTM Int., **1**(8), p. JAI11563; also published in "Probabilistic Aspects of Life Prediction," ASTM STP 1450, pp. 199–215.

[9] McClung, R. C., Enright, M. P., Lee, Y.-D., Huyse, L., and Fitch, S. H. K., 2004, "Efficient Fracture Design for Complex Turbine Engine Components," *Proceedings of the 49th ASME International Gas Turbine and Aeroengine Technical Congress*, Vienna, Austria, June 14–17.
[10] Enright, M. P., Huyse, L., McClung, R. C., and Millwater, H. R., 2004, "Probabilistic Methodology for Life Prediction of Aircraft Turbine Rotors," *Proceedings of the 9th Biennial ASCE Aerospace Division International Conference on Engineering, Construction and Operations in Challenging Environments (Earth and Space 2004)*, R. B. Malla, and A. Maji, eds., ASCE, Houston, TX, Mar. 7–10, ASCE, Reston, VA, pp. 453–460.
[11] Grison, J., and Remy, L., 1997, "Fatigue Failure Probability in a Powder Metallurgy Ni-Base Superalloy," Eng. Fract. Mech., **57**(1), pp. 41–55.
[12] Drar, H., 2001, "Stages of Fatigue Fracture in Nickel Alloyed Powder Metallurgy Steel," Mater. Sci. Technol., **17**, pp. 1259–1264.
[13] Bannantine, J. A., Comer, J. J., and Handrock, J. L., 1990, *Fundamentals of Metal Fatigue Analysis*, Prentice-Hall, Englewood Cliffs, NJ, pp. 69–70.
[14] Hicks, M. A., and Pickard, A. C., 1988, "Life Prediction in Turbine Engines and the Role of Small Cracks," Mater. Sci. Eng., A, **103**, pp. 43–48.
[15] McClung, R. C., Francis, W. L., and Hudak, S. J., 2006, "A New Approach to Fatigue Life Prediction Based on Nucleation and Growth," Fatigue 2006, Ninth International Fatigue Congress, Atlanta, GA, May.
[16] Smith, K. N., Watson, P., and Topper, T. H., 1970, "A Stress-Strain Function for the Fatigue of Metals," J. Mater., **5**(4), pp. 767–778.
[17] Ayyub, B. M., and McCuen, R. H., 2003, *Probability, Statistics, and Reliability for Engineers and Scientists*, Chapman and Hall, New York, pp. 413–414.
[18] Haldar, A., and Mahadevan, S., 2000, *Probability, Reliability, and Statistical Methods in Engineering Design*, Wiley, New York, pp. 149–150.
[19] Enright, M. P., McClung, R. C., and Huyse, L., 2005, "A Probabilistic Framework for Risk Prediction of Engine Components With Inherent and Induced Material Anomalies," *Proceedings of the 50th ASME International Gas Turbine and Aeroengine Technical Congress*, Reno, NV, Jun. 6–9.
[20] Enright, M. P., and Huyse, L., 2005, "Methodology for Probabilistic Life Prediction of Multiple Anomaly Materials," *Proceedings of the 46th AIAA Structures, Structural Dynamics, and Materials Conference*, AIAA, Austin, TX, Apr. 18–21.
[21] Enright, M. P., McClung, R. C., and Huyse, L., 2005, "Fracture Mechanics-Based Probabilistic Life Prediction of Components With Large Numbers of Inherent Material Anomalies," *Proceedings of the 9th International Conference on Structural Safety and Reliability (ICOSSAR)*, Rome, Italy, Jun. 19–22, pp. 601–607.
[22] El Haddad, M. H., Smith, K. N., and Topper, T. H., 1979, "Fatigue Crack Propagation of Short Cracks," ASME J. Eng. Mater. Technol., **101**, pp. 42–46.
[23] Gallagher, J. P., 1999, "Improved High Cycle Fatigue (HCF) Life Prediction," UDRI Report No. UDR-TR-1999-00079.
[24] Raizenne, M. D., 1987, "Fatigue Crack Growth Rate Data for AGARD TX114 Engine Disc Cooperative Test Programme," *Laboratory Memorandum ST-479*, National Aeronautical Establishment, Ottawa, Canada.
[25] Mom, A. J. A., and Raizenne, M. D., 1988, "AGARD Engine Disc Cooperative Test Programme," AGARD Report No. 766.
[26] Southwest Research Institute, 2004, *DARWIN® User's Guide*, Southwest Research Institute, San Antonio, TX.